

Distributed Arithmetic Coding for the Slepian-Wolf problem

Marco Grangetto, *Member, IEEE*, Enrico Magli, *Senior Member, IEEE*, Gabriella Olmo, *Senior Member, IEEE*

EDICS: SEN-DCSC, SPC-CODC

Abstract

Distributed source coding schemes are typically based on the use of channels codes as source codes. In this paper we propose a new paradigm, named “distributed arithmetic coding”, which extends arithmetic codes to the distributed case employing sequential decoding aided by the side information. In particular, we introduce a distributed binary arithmetic coder for the Slepian-Wolf coding problem, along with a joint decoder. The proposed scheme can be applied to two sources in both the asymmetric mode, wherein one source acts as side information, and the symmetric mode, wherein both sources are coded with ambiguity, at any combination of achievable rates. Distributed arithmetic coding provides several advantages over existing Slepian-Wolf coders, especially good performance at small block lengths, and the ability to incorporate arbitrary source models in the encoding process, e.g., context-based statistical models, in much the same way as a classical arithmetic coder. We have compared the performance of distributed arithmetic coding with turbo codes and low-density parity-check codes, and found that the proposed approach is very competitive.

Index Terms

Distributed source coding, arithmetic coding, Slepian-Wolf coding, Wyner-Ziv coding, compression, turbo codes, LDPC codes.

M. Grangetto is with Dip. di Informatica, Università degli Studi di Torino, Corso Svizzera 185 - 10149 Torino - ITALY - Ph.: +39-011-6706711 - FAX: +39-011-751603 - E-mail: marco.grangetto@di.unito.it

E. Magli and G. Olmo are with Dip. di Elettronica, Politecnico di Torino, Corso Duca degli Abruzzi 24 - 10129 Torino - Italy - Ph.: +39-011-5644195 - FAX: +39-011-5644099 - E-mail: enrico.magli (gabriella.olmo)@polito.it.
Corresponding author: Enrico Magli.

Distributed Arithmetic Coding for the Slepian-Wolf problem

I. INTRODUCTION AND BACKGROUND

In recent years, distributed source coding (DSC) has received an increasing attention from the signal processing community. DSC considers a situation in which two (or more) statistically dependent sources X and Y must be encoded by separate encoders that are not allowed to talk to each other. Performing separate lossless compression may seem less efficient than joint encoding. However, DSC theory proves that, under certain assumptions, separate encoding is optimal, provided that the sources are decoded jointly [1]. For example, with two sources it is possible to perform “standard” encoding of the first source (called *side information*) at a rate equal to its entropy, and “conditional” encoding of the second one at a rate lower than its entropy, with no information about the first source available at the second encoder; we refer to this as “asymmetric” Slepian-Wolf (S-W) problem. Alternatively, both sources can be encoded at a rate smaller than their respective entropy, and decoded jointly, which we refer to as “symmetric” S-W coding.

DSC theory also encompasses lossy compression [2]; it has been shown that, under certain conditions, there is no performance loss in using DSC [2], [3], and that possible losses are bounded below 0.5 bit per sample (bps) for quadratic distortion metric [4]. In practice, lossy DSC is typically implemented using a quantizer followed by lossless DSC, while the decoder consists of the joint decoder followed by a joint dequantizer. Lossless and lossy DSC have several potential applications, e.g., coding for non co-located sources such as sensor networks, distributed video coding [5], [6], [7], [8], layered video coding [9], [10], error resilient video coding [11], and satellite image coding [12], [13], just to mention a few. The interested reader is referred to [14] for an excellent tutorial.

Traditional entropy coding of an information source can be performed using one out of many available methods, the most popular being arithmetic coding (AC) and Huffman coding. “Conditional” (i.e., DSC) coders are typically implemented using channel codes, by representing the source using the syndrome or the parity bits of a suitable channel code of given rate. The syndrome identifies sets of codewords (“cosets”) with maximum distance properties, so that decoding an ambiguous description of a source at a rate less than its entropy (given the side information) incurs minimum error probability. If the correlation between X and Y can be modeled as a “virtual” channel described as $X = Y + W$, with W an additive noise process, a good channel code for that transmission problem is also expected to be a good S-W source code [3].

Regarding asymmetric S-W coding, the first practical technique has been described in [15], and employs trellis codes. Recently, more powerful channel codes such as turbo codes have been proposed in [6], [16], [17], and low-density parity-check (LDPC) [18] codes have been used in [19], [20], [21]. Turbo and LDPC codes can get extremely close to channel capacity, although they require the block size to be rather large. Note that the constituent codes of turbo-codes are convolutional codes, hence the syndrome is difficult to compute. In [6] the cosets are formed by all messages that produce the same parity bits, even though this approach is somewhat suboptimal [17], since the geometrical properties of these cosets are not as good as those of syndrome-based coding. In [22] a syndrome former is used to deal with this problem. Multilevel codes have also been addressed; in [23] trellis codes are extended to multilevel sources, whereas in [24] a similar approach is proposed for LDPC codes.

Besides techniques based on channel coding, a few authors have also investigated the use of source coders for DSC. This is motivated by the fact that existing source coders obviously exhibit nice compression features that should be retained in a DSC coder, such as the ability to employ flexible and adaptive probability models, and low encoding complexity. In [25] the problem of designing a variable-length DSC coder is addressed; it is shown that the problem of designing a zero-error such coder is NP-hard. In [26] a similar approach is followed; the authors consider the problem of designing Huffman and arithmetic DSC coders for multilevel sources with zero or almost-zero error probability. The idea is that, if the joint density of the source and the side information satisfies certain conditions, the same codeword (or the same interval for the AC process) can be associated to multiple symbols. This approach leads to an encoder with a complex modeling stage (NP-hard for the optimal code, though suboptimal polynomial-time algorithms are provided in [26]), while the decoding process resembles a classical arithmetic decoder.

As for symmetric S-W codes, a few techniques have been recently proposed. A symmetric code can be obtained from an asymmetric one through time sharing, whereby the two sources alternatively take the role of the source and the side information; however, current DSC coders cannot easily accommodate this approach. Syndrome-based channel code partitioning has been introduced in [27], and extended in [28] to systematic codes. A similar technique is described in [29], encompassing non-systematic codes. Syndrome formers have also been proposed for symmetric S-W coding [30]. Moreover, techniques based on the use of parity bits can also be employed, as they can typically provide rate compatibility. A practical code has been proposed in [16] using two turbo codes that are decoded jointly, achieving the equal rate point; in [31] an algorithm is introduced that employs turbo codes to achieve arbitrary rate splitting. Symmetric S-W codes based on LDPC codes have also been developed [32], [33].

Although several near-optimal DSC coders have been designed for simple ideal sources (e.g., binary and Gaussian sources), the applications of practical DSC schemes to realistic signals typically incurs the following problems.

- Channel codes get very close to capacity only for very large data blocks (typically in excess of 10^5 symbols). In many applications, however, the basic units to be encoded are of the order of a few hundreds to a few thousands symbols. For such block lengths, channel codes have good but not optimal performance.
- The symbols contained in a block are expected to follow a stationary statistical distribution. However, typical real-world sources are not stationary. This calls for either the use of short blocks, which weakens the performance of the S-W coder, or the estimation of conditional probabilities over contexts, which cannot be easily accommodated by existing S-W coders.
- When the sources are strongly correlated (i.e., in the most favorable case), very high-rate channel codes are needed (e.g., rate- $\frac{99}{100}$ codes). However, capacity-achieving channel codes are often not very efficient at high rate.
- In those applications where DSC is used to limit the encoder complexity, it should be noted that the complexity of existing S-W coders is not negligible, and often higher than that of existing non-DSC coders. This seriously weakens the benefits of DSC.
- Upgrading an existing compression algorithm like JPEG 2000 or H.264/AVC to provide DSC functionalities requires at least to redesign the entropy coding stage, adopting one of the existing DSC schemes.

Among these issues, the block length is particularly important. While it has been shown that, on ideal sources with very large block length, the performance of some practical DSC coders can be as close as 0.09 bits to the theoretical limit [14], so far DSC of real-world data has fallen short of its expectations, one reason being the necessity to employ much smaller blocks. For example, the PRISM video coder [5] encodes each macroblock independently, with a block length of 256 samples. For the coder in [6], the block length is equal to the number of 8x8 blocks in one picture (1584 for the CIF format). The performance of both coders is rather far from optimal, highlighting the need of DSC coders for realistic block lengths.

A solution to this problem has been introduced in [34], where an extension of AC, named distributed arithmetic coding (DAC), has been proposed for asymmetric S-W coding. Moreover, in [35] DAC has been extended to the case of symmetric S-W coding of two sources at the same rate (i.e., the mid-point of the S-W rate region). DAC and its decoding process do not currently have a rigorous mathematical theory that proves they can asymptotically achieve the S-W rate region; such theory is

very difficult to develop because of the non-linearity of AC. However, DAC is a practical algorithm that was shown in [34] to outperform other existing distributed coders. In this paper, we build on the results presented in [34], providing several new contributions. For asymmetric coding, we focus on i.i.d. sources as these are often found in many DSC applications; for example, in transform-domain distributed video coding, DAC could be applied to the bit-planes of transform coefficients, which can be modeled as i.i.d. We optimize the DAC using an improved encoder termination procedure, and we investigate the rate allocation problem, i.e., how to optimally select the encoding parameters to achieve a desired target rate. We evaluate the performance of this new design comparing it with turbo and LDPC codes, including the case of extremely correlated sources with highly skewed probabilities. This is of interest in multimedia applications because the most significant bit-planes of the transform coefficients of an image or video sequence are almost always equal to zero, and are strongly correlated with the side information. For symmetric coding, we extend our previous work in [35] by introducing DAC encoding and rate allocation procedures that allow to encode an arbitrary number of sources with arbitrary combination of rates. We develop and test the decoder for two sources.

Finally, it should be noted that an asymmetric DAC scheme has been independently and concurrently developed in [36] using quasi-arithmetic codes. Quasi-arithmetic codes are a low-complexity approximation to arithmetic codes, providing smaller encoding and decoding complexity [37]. These codes allow the interval endpoints to be only a finite set of points. While this yields suboptimal compression performance, it makes the arithmetic coder a finite state machine, simplifying the decoding process with side information.

This paper is organized as follows. In Sect. III we describe the DAC encoding process for the asymmetric case, in Sect. III we describe the DAC decoder, and in Sect. IV we study the rate allocation and parameter selection problem. In Sect. V we describe the DAC encoder, decoder and rate allocator for the symmetric case. In Sect. VI and VII we report the DAC performance evaluation results in the asymmetric and symmetric case respectively. Finally, in Sect. VIII we draw some conclusions.

II. DISTRIBUTED ARITHMETIC CODING: ASYMMETRIC ENCODER

Before describing the DAC encoder, it should be noted that the AC process typically consists of a modeling stage and a coding stage. The modeling stage has the purpose of computing the parameters of a suitable statistical model of the source, in terms of the probability that a given bit takes on value 0 or 1. This model can be arbitrarily sophisticated, e.g., by using contexts, adaptive probability estimation, and so forth. The coding stage takes the probabilities as input, and implements the actual AC procedure, which outputs a binary codeword describing the input sequence.

Let X be a binary memoryless source that emits a semi-infinite sequence of random variables X_i , $i = 0, 1, \dots$, with probabilities $p_0^X = P(X_i = 0)$ and $p_1^X = P(X_i = 1)$. We are concerned with encoding the sequence $\underline{x} = [x_0, \dots, x_{N-1}]$ consisting in the first N occurrences of this source. The modeling and coding stages are shown in Fig. 1-a. The modeling stage takes as input the sequence \underline{x} , and outputs an estimate of the probabilities p_0^X and p_1^X . The coding stage takes as input \underline{x} , p_0^X and p_1^X , and generates a codeword C_X . The expected length of C_X depends on p_0^X and p_1^X , and is determined once these probabilities are given.

In order to use the DAC, we consider two sources X and Y , where Y is a binary memoryless source that emits random variables Y_i , $i = 0, 1, \dots$, with probabilities $p_0^Y = P(Y_i = 0)$ and $p_1^Y = P(Y_i = 1)$. The first N occurrences of this source form the side information $\underline{y} = [y_0, \dots, y_{N-1}]$. We assume that X and Y are i.i.d. sources, and that X_i and Y_i are statistically dependent for a given i . The entropy of X is defined as $H(X) = -\sum_{j=0}^1 p_j^X \log_2 p_j^X$, and similarly for Y . The conditional entropy of X given Y is defined as $H(X|Y) = -\sum_{j=0}^1 \sum_{k=0}^1 P(X_i = j, Y_i = k) \log_2 P(X_i = j|Y_i = k)$.

For DAC, three blocks can be identified, as in Fig. 1-b, namely the modeling, rate allocation, and coding stages. The modeling stage is exactly the same as in the classical AC. The coding stage will be described in Sect. II-B; it takes as inputs \underline{x} , the probabilities p_0^X and p_1^X , and the parameter k^X , and outputs a codeword C'_X . Unlike a classical AC, where the expected rate is function of the source probabilities, and hence cannot be selected *a priori*, the DAC allows to select any desired rate not larger than the expected rate of a classical AC. This is very important, since in a DSC setting the rate for \underline{x} should depend not only on how much “compressible” the source is, but also on how much correlated X_i and Y_i are. For this reason, in DAC we also have a rate allocation stage that takes as input the probabilities p_0^X and p_1^X and the conditional entropy $H(X|Y)$, and outputs a parameter k^X that drives the DAC coding stage to achieve the desired target rate.

In this paper we deal with the coding and rate allocation stages, and assume that the input probabilities p_0^X , p_1^X and conditional entropy $H(X|Y)$ are known *a priori*. This allows us to focus on the distributed coding aspects of the proposed scheme, and, at the same time, keeps the scheme independent of the modeling stage.

A. Arithmetic coding

We first review the classical AC coding process, as this sets the stage for the description of the DAC encoder; an overview can be found in [38]. The binary AC process for \underline{x} is based on the probabilities p_0^X and p_1^X , which are used to partition the $[0, 1)$ interval into sub-intervals associated to possible occurrences of the input symbols. At initialization the “current” interval is set to $I_0 = [0, 1)$. For each input symbol x_i , the current interval I_i is partitioned into two adjacent sub-intervals of lengths

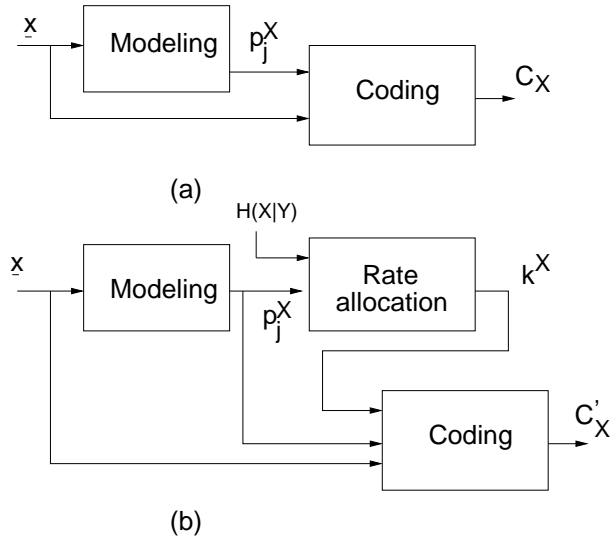


Fig. 1. Modeling, rate allocation and coding stage for (a) classical AC, and (b) DAC.

$p_0^X |I_i|$ and $p_1^X |I_i|$, where $|I_i|$ is the length of I_i . The sub-interval corresponding to the actual value of x_i is selected as the next current interval I_{i+1} , and this procedure is repeated for the next symbol. After all N symbols have been processed, the sequence is represented by the final interval I_N . The codeword C_X can consist in the binary representation of any number inside I_N (e.g., the number in I_N with the shortest binary representation), and requires approximately $-\log_2 |I_N|$ bits.

B. DAC encoder

Similarly to other S-W coders, DAC is based on the principle of inserting some ambiguity in the source description during the encoding process. This is obtained using a modified interval subdivision strategy. In particular, the DAC employs a set of intervals whose lengths are proportional to the modified probabilities \tilde{p}_0^X and \tilde{p}_1^X , such that $\tilde{p}_0^X \geq p_0^X$ and $\tilde{p}_1^X \geq p_1^X$. In order to fit the enlarged sub-intervals into the $[0, 1)$ interval, they are allowed to partially overlap. This prevents the decoder from discriminating the correct interval, unless the side information is used.

The detailed DAC encoding procedure is described in the following. At initialization the “current” interval is set to $I'_0 = [0, 1)$. For each input symbol x_i , the current interval I'_i is subdivided into two partially overlapped sub-intervals whose lengths are $\tilde{p}_0^X |I'_i|$ and $\tilde{p}_1^X |I'_i|$. The interval representing symbol x_i is selected as the next current interval I'_{i+1} . After all N symbols have been processed, the sequence is represented by the final interval I'_N . The codeword C'_X can consist in the binary representation of any number inside I'_N , and requires approximately $-\log_2 |I'_N|$ bits. This procedure is sketched in Fig. 2. At the decoder side, whenever the codeword points to an overlapped region, the input symbol cannot be detected unambiguously, and additional information must be exploited

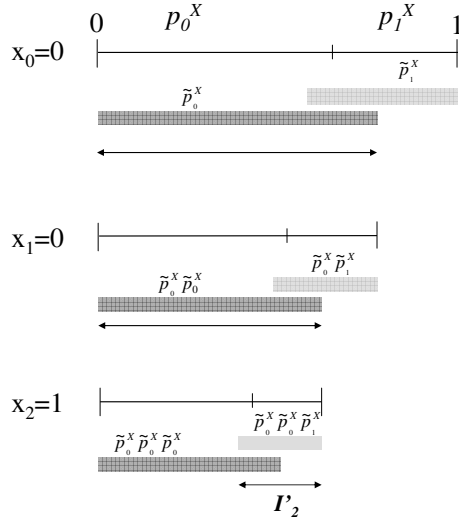


Fig. 2. Distributed arithmetic encoding procedure for a block of three symbols.

by the joint decoder to solve the ambiguity. It is worth noticing that the DAC encoding procedure is a generalization of AC. Letting $\tilde{p}_0^X = p_0^X$ and $\tilde{p}_1^X = p_1^X$ leads to the AC encoding process described in Sect. II-A, with $I'_N = I_N$ and $C'_X = C_X$.

It should also be noted that, for simplicity, the description of the AC and DAC provided above assumes infinite precision arithmetic. The practical implementation used in Sect. VI and VII employs fixed-point arithmetic and interval renormalization.

III. DECODING FOR THE ASYMMETRIC CASE

The objective of the DAC decoder is joint decoding of the sequence \underline{x} given the correlated side information \underline{y} . The arithmetic decoding machinery of the DAC decoder presents limited modifications with respect to standard arithmetic decoders; a fixed-point implementation has been employed, with the same interval scaling and overlapping rules used at the encoder. In the following the arithmetic decoder state at the i -th decoding step is denoted as $\sigma_i, i = 0, \dots, N - 1$. The data stored in σ_i represent the interval I'_i and the codeword at iteration i .

The decoding process can be formulated as a symbol-driven sequential search along a proper decoding tree, where each node represents a state σ_i , and a path in the tree represents a possible decoded sequence. The following elementary decoding functions are required to explore the tree:

- $(\tilde{x}_i, \sigma_{i+1}) = \text{Test-One-Symbol}(\sigma_i)$: it computes the sub-intervals at the i -th step, compares them with C'_X and outputs either an unambiguous symbol $\tilde{x}_i = 0, 1$ (if C'_X belongs to one of the non-overlapped regions), or an ambiguous symbol $\tilde{x}_i = A$. In case of unambiguous decoding, the new decoder state σ_{i+1} is returned for the following iterations.

- $\sigma_{i+1} = \text{Force-One-Symbol}(\sigma_i, \tilde{x}_i)$: it forces the decoder to select the sub-interval corresponding to the symbol \tilde{x}_i regardless of the ambiguity; the updated decoder state is returned.

In Fig. 3 an example of a section of the decoding tree is shown. In this example the decoder is not able to make a decision on the i -th symbol, as *Test-One-Symbol* returns $\tilde{x}_i = A$. As a consequence, two alternative decoding attempts are pursued by calling *Force-One-Symbol* with $\tilde{x}_i = 0, 1$ respectively. In principle, by iterating this process, the tree \mathcal{T} , representing all the possible decoded sequences, can be explored. The best decoded sequence can finally be selected applying the *Maximum A Posteriori* (MAP) criterion $\hat{\underline{x}} = \arg \max_{\mathcal{T}} P(X_0, \dots, X_{N-1} | C'_X, Y)$.

In general, exhaustive search cannot be applied due to the exponential growth of \mathcal{T} . A viable solution is obtained applying the breadth-first sequential search known as M -algorithm [39], [40]; at each tree depth, only the M nodes with the best partial metric are retained. This amounts to visiting only a subset of the most likely paths in \mathcal{T} . The MAP metric for a given node can be evaluated as follows:

$$P(X_0 = \tilde{x}_0, \dots, X_i = \tilde{x}_i | C'_X, Y) = \prod_{j=0}^i P(X_j = \tilde{x}_j | C'_X, Y_j) \quad (1)$$

Metric (1) can be expressed into additive terms by setting:

$$\begin{aligned} \Lambda_{i+1} &\triangleq \log P(X_0 = \tilde{x}_0, \dots, X_i = \tilde{x}_i | C'_X, Y) = \sum_{j=0}^i \lambda_j \\ \lambda_j &\triangleq \log P(X_j = \tilde{x}_j | C'_X, Y_j) \end{aligned} \quad (2)$$

where $\Lambda_0 = 0$ and λ_i represent the additive metric to be associated to each branch of \mathcal{T} .

The pseudocode for the DAC decoder is given in Algorithm 1, where \mathcal{T}_i represents the list of nodes in \mathcal{T} explored at depth i ; each tree node stores its corresponding arithmetic decoder state σ_i and the accumulated metric Λ_i .

It is worth pointing out that M has to be selected as a trade-off between the memory/complexity requirements and the error probability, i.e., the probability that the path corresponding to the original sequence \underline{x} is accidentally dropped. As in the case of standard Viterbi decoding, the path metric turns out to be stable and reliable as long as a significant amount of terms, i.e., number of decoded symbols \tilde{x}_i , are taken into account. In the pessimistic case when all symbol positions i trigger a decoder branching, given M , one can guarantee that at least $\log_2(M)$ symbols are considered for metric comparisons and pruning. On the other hand, in practical cases, the interval overlap is only partial and branching does not occur at every symbol iteration. All the experimental results presented in Sect. VI have been obtained using $M = 2048$, while the trade-off between performance and complexity is analyzed in Sect. VI-F.

Algorithm 1 DAC decoder (asymmetric case)

```

Initialize  $\mathcal{T}_0$  with root node  $(\sigma_0, \Lambda_0 = 0)$ 
Set symbol counter  $i \leftarrow 0$ 
while  $(i < N)$  do
  for All nodes  $(\sigma_i, \Lambda_i)$  in  $\mathcal{T}_i$  do
     $(\tilde{x}_i, \sigma_{i+1}) = \text{Test-One-Symbol}(\sigma_i)$ 
    if  $\tilde{x}_i = A$  then
      for  $k = (0, 1)$  do
         $\sigma_{i+1} = \text{Force-One-Symbol}(\sigma_i, \tilde{x}_i = k)$ 
         $\Lambda_{i+1} \leftarrow \Lambda_i + \lambda_i$ 
        Insert  $(\sigma_{i+1}, \Lambda_{i+1})$  in  $\mathcal{T}_{i+1}$ 
      end for
    else
       $\Lambda_{i+1} \leftarrow \Lambda_i + \lambda_i$ 
      Insert  $(\sigma_{i+1}, \Lambda_{i+1})$  in  $\mathcal{T}_{i+1}$ 
    end if
  end for
  Sort nodes in  $\mathcal{T}_{i+1}$  according to metric  $\Lambda_{i+1}$ 
  Keep only the  $M$  nodes with best metric in  $\mathcal{T}_{i+1}$ 
end while
Output  $\tilde{x}$  (sequence corresponding to the first node stored in  $\mathcal{T}_N$ )

```

Finally, metric reliability cannot be guaranteed for the very last symbols of a finite-length sequence \underline{x} . For channel codes, e.g., convolutional codes, this issue is tackled by imposing a proper termination strategy, e.g., forcing the encoded sequence to end in the first state of the trellis. A similar approach is necessary when using DAC. Examples of AC termination strategies are encoding a known termination pattern or end-of-block symbol with a certain probability or, in the case of context-based AC, driving the AC encoder in a given context. For DAC, we employ a new termination policy that is tailored to its particular features. In particular, termination is obtained by encoding the last T symbols of the sequence without interval overlap, i.e., using $\tilde{p}_j^X = p_j^X$, for all symbols x_i with $i \geq N - T$. As a consequence, no nodes in the DAC decoding tree will cause branching in the last T steps, making the final metrics more reliable for the selection of the most likely sequence. However, there is a rate penalty for the termination symbols.

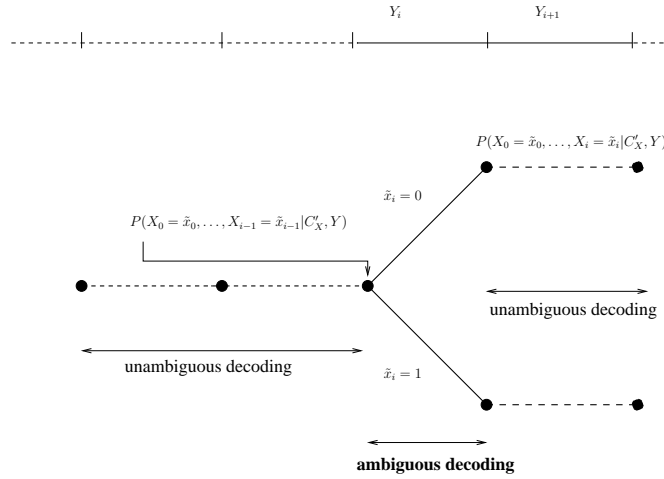


Fig. 3. Distributed arithmetic decoding tree for asymmetric S-W coding.

IV. RATE ALLOCATION AND CHOICE OF THE OVERLAP FACTOR

The length of codeword C'_X is determined by the length $|I'_N|$ of the final interval, which in turn depends on how much \tilde{p}_0^X and \tilde{p}_1^X are larger than p_0^X and p_1^X . As a consequence, in order to select the desired rate, it is important to quantitatively determine the dependence of the expected rate on the overlap, because this will drive the selection of the desired amount of overlap. Moreover, we also need to understand how to split the overlap in order to achieve good decoding performance. In the following we derive the expected rate obtained by the DAC as a function of the set of input probabilities and the amount of overlap.

A. Calculation of the rate yielded by DAC

We are interested in finding the expected rate \tilde{R} (in bps) of the codeword used by the DAC to encode the sequence \underline{x} . This is given by the following formula:

$$\tilde{R} = \sum_{j=0}^1 p_j^X \log_2 \frac{1}{\tilde{p}_j^X} \quad (3)$$

This can be derived straightforwardly from the property that the codeword generated by an AC has an expected length that depends on the size of the final interval, that is, on the product of the probabilities \tilde{p}_j^X , and hence on the amount of overlap. The expectation is computed using the true probabilities p_j^X .

We set $\tilde{p}_j^X = \alpha_j^X p_j^X$, where $\alpha_j^X \geq 1$, so that $\tilde{p}_0^X + \tilde{p}_1^X \geq 1$. This amounts to enlarging each interval by an amount proportional to the overlap factors α_j^X . The expected rate achieved by the

DAC becomes

$$\tilde{R} = \sum_{j=0}^1 p_j^X (r_j^X - \delta_j^X)$$

where $r_j^X = -\log_2 p_j^X$, and $\delta_j^X = \log_2 \alpha_j^X$. Note that r_j^X represents the rate contribution of symbol j yielded by standard AC, while δ_j^X represents the decrease of this contribution, i.e., the average number of bits saved in the binary representation of the j -th input symbol.

B. Design of the overlap factors

Once a target rate has been selected, the problem arises of selecting α_j^X . As an example, a possible choice is to take equal overlap factors $\alpha_0^X = \alpha_1^X = \alpha^X$. This implies that each interval is enlarged by a factor α^X that does not depend on the source probability p_j^X . This leads to a target rate

$$R'_X = H(X) - \log_2 \alpha^X. \quad (4)$$

It can be shown that this choice minimizes the rate \tilde{R} for a given total amount of overlap $\alpha_0^X p_0^X + \alpha_1^X p_1^X - 1$; the computations are simple and are omitted for brevity. This choice is not necessarily optimal in terms of the decoder error probability. However, optimizing for the error probability is impractical because of the nonlinearity of the arithmetic coding process.

In practice, one also has to make sure that the enlarged intervals $[0, \alpha_0^X p_0^X)$ and $[1 - \alpha_1^X p_1^X, 1)$ are both contained inside the $[0, 1)$ interval. E.g., taking equal overlap factors as above does not guarantee this. We have devised the following rule that allows to achieve any desired rate satisfying the constraint above. We apply the following constraint:

$$\frac{\delta_j^X}{r_j^X} = k^X \quad (5)$$

with k^X a positive constant independent of j . This leads to

$$\alpha_j^X = (p_j^X)^{-k^X} \quad (6)$$

This can be interpreted as an additional constraint that the rate reduction for symbols “0” and “1” depends on their probabilities, i.e., the least probable symbol undergoes a larger reduction. Using (6), it can be easily shown that the expected rate achieved by the DAC can be written as

$$\tilde{R} = (1 - k^X) H(X). \quad (7)$$

Thus, the allocation problem for an i.i.d. source is very simple. We assume that the conditional entropy $H(X|Y)$ is available as in Fig. 1-b, modeling the correlation between X and Y . In asymmetric DSC, \underline{x} should be ideally coded at a rate arbitrarily close to $H(X|Y)$. In practice, due to the suboptimality of any practical coder, some margin $\mu \geq 1$ should be taken. Hence, we assume that

the allocation problem can be written as $(1 - k^X)H(X) \leq \mu H(X|Y)$. Since μ is a constant and $H(X|Y)$ and $H(X)$ are given, one can solve for k^X and then perform the encoding process.

Finally, it should be noted that, while we have assumed that X and Y are i.i.d., the DAC concept can be easily extended to a nonstationary source. This simply requires to consider all probabilities and overlap factors as depending on index i ; all computations, including the design of the overlap factors and the derivation of the target rate, can be extended straightforwardly. A possible application is represented by context-based coding or Markov modeling of correlated sources. There is one caveat though, in that, if the probabilities and context of each symbol are computed by the decoder from past symbols, decoding errors can generate significant error propagation.

V. DISTRIBUTED ARITHMETIC CODING: THE SYMMETRIC CASE

A. Symmetric DAC encoding and rate allocation

In many applications, it is preferable to encode the correlated sources at similar rather than unbalanced rates; in this case, symmetric S-W coding can be used. Considering a pair of sources, in symmetric S-W coding both X and Y are encoded using separate DACs. We denote as C'_X and C'_Y the codewords representing X and Y , and R'_X and R'_Y the respective rates. With DAC, the rate of X and Y can be adjusted with a proper selection of the parameters k^X and k^Y for the two DAC encoders. However, it should be noted that, for the same total rate, not all possible choices of k^X and k^Y are equally good, because some of them could complicate the decoder design, or be suboptimal in terms of error probability. To highlight the potential problems of a straightforward extension of the asymmetric DAC, let us assume that k^X and k^Y can be chosen arbitrarily. This would require a decoder that performs a search in a symbol-synchronous tree where each node represents *two* sequential decoder states (σ_i^X, σ_i^Y) for X and Y respectively. If the interval selection is ambiguous for both sequences, the four possible binary symbol pairs (00,01,10,11) need to be included in the search space; this would accelerate the exponential growth of the tree, and quickly make the decoder search unfeasible. This example shows that some constraints need to be put on k^X and k^Y in order to limit the growth rate of the search space.

To overcome this problem, we propose an algorithm that applies the idea of time-sharing to the DAC. The concept of time-shared DAC has been preliminarily presented in [35] for a pair of sources in the subcase $R'_X = R'_Y$, i.e. providing only the mid-point of the S-W rate region. In the following we extend this to an arbitrary combination of rates, and show how this can be generalized to an arbitrary number of sources. For two sources, the idea is to divide the set of input indexes $i = 0, 1, \dots, N - 1$ in two disjoint sets such that, at each index i , ambiguity is introduced in at most one out of the two sources. In particular, for sequences \underline{x} and \underline{y} of length N , let \mathcal{A}_X and \mathcal{A}_Y be the subsets of even and

odd integer numbers in $\{0, \dots, N - 1\}$ respectively. We employ a DAC on \underline{x} and \underline{y} , but the choice of parameters k^X and k^Y differs. In particular, we let the parameters depend on the symbol index i , i.e., k_i^X and k_i^Y . The DAC of \underline{x} employs parameter $k_i^X = k^X \geq 0$ for all $i \in \mathcal{A}_X$, and $k_i^X = 0$ otherwise. Vice versa, \underline{y} is encoded with parameter $k_i^Y = k^Y \geq 0$ for all $i \in \mathcal{A}_Y$, and $k_i^Y = 0$ otherwise. As a consequence of these constraints, at each step of the decoding process, ambiguity appears in at most one out the two sequences. In this way, the growth rate of the decoding tree remains manageable, as no more than two new states are generated at each transition, exactly as in the asymmetric DAC decoder; this also makes the MAP metric simpler. The conceptual relation with time-sharing is evident. Since, during the DAC encoding process, for each input symbol the ambiguity is introduced in at most one out the two encoders, this corresponds to switching the role of side information between either source on a symbol-by-symbol basis.

By varying the parameters k^X and k^Y , all combinations of rates can be achieved. The achieved rates can be derived repeating the same computations described in Sect. IV, and can be expressed as $R'_X = \left(1 - \frac{k^X}{2}\right) H(X)$ and $R'_Y = \left(1 - \frac{k^Y}{2}\right) H(Y)$. The rate allocation problem amounts to selecting suitable rates R'_X and R'_Y such that $R'_X \geq H(X|Y)$, $R'_Y \geq H(Y|X)$, and $R'_X + R'_Y \geq H(X, Y)$. In practice one will typically take some margin $\mu \geq 1$, such that $R'_X + R'_Y = \mu H(X, Y)$; for safety, a margin should also be taken on R'_X and R'_Y with respect to the conditional entropy. Since the prior probabilities of X and Y are given, one can solve for k^X and k^Y , and then perform the encoding process. Thus, the whole S-W rate region can be swept.

B. Decoding process for symmetric DAC

Similarly to the asymmetric case, the symmetric decoding process can be viewed as a search along a tree; however, specifically for the case of two correlated sources, each node in tree represents the decoding states (σ_i^X, σ_i^Y) of two sequential arithmetic decoders for \underline{x} and \underline{y} respectively. At each iteration, sequential decoding is run from both states. The time-sharing approach guarantees that, for a given index i , the ambiguity can be found only in one of the two decoders. Therefore, at most two branches must be considered, and the tree can be constructed using the same functions introduced in Sect. III for the asymmetric case. This would be the same also for P sources. In particular, for $i \in \mathcal{A}_X$, *Test-One-Symbol* (σ_i^Y) yields an unambiguous symbol $\tilde{y}_i \neq A$, whereas ambiguity can be found only while attempting decoding for \underline{x} with *Test-One-Symbol* (σ_i^X) . In conclusion, from the node (σ_i^X, σ_i^Y) the function *Test-One-Symbol* is used on both states. If ambiguity is found on \tilde{x}_i , *Force-One-Symbol* is then used to explore the two alternative paths for \tilde{x}_i , whereas \tilde{y}_i is used as side information for branch metric evaluation. In the case that $i \in \mathcal{A}_Y$, the roles of \underline{x} and \underline{y} are exchanged. Therefore, Algorithm 1 can be easily extended to the symmetric case by alternatively probing either \underline{x} or \underline{y} for

ambiguity, and possibly generating a branching. The joint probability distribution can be written as

$$P(X_0 = \tilde{x}_0, \dots, X_{N-1} = \tilde{x}_{N-1}, Y_0 = \tilde{y}_0, \dots, Y_{N-1} = \tilde{y}_{N-1} | C'_X, C'_Y) = \quad (8)$$

$$= \prod_{i \in \mathcal{A}_X} P(X_i = \tilde{x}_i | Y_i, C'_X, C'_Y) \prod_{i \in \mathcal{A}_Y} P(Y_i = \tilde{y}_i | X_i, C'_X, C'_Y)$$

The symmetric encoder and decoder can be easily generalized to an arbitrary number P of sources. The idea is to identify P subsets of input indexes $i = 0, 1, \dots, N-1$ such that, at each symbol index i , ambiguity is introduced in at most one out of the P sources. In particular, for sequences $\underline{x}^{(1)}, \dots, \underline{x}^{(P)}$ of length N , let $\mathcal{A}_1, \dots, \mathcal{A}_P$ be disjoint subsets of $\{0, 1, \dots, N-1\}$. We denote the DAC parameters as $k_i^{(1)}, \dots, k_i^{(P)}$. The DAC of $\underline{x}^{(j)}$ employs parameter $k_i^{(j)} = k^{(j)} \geq 0$ for all $i \in \mathcal{A}_j$, and $k_i^{(j)} = 0$ otherwise. As a consequence of these constraints, at each step of the decoding process, ambiguity appears in at most one out the P sequences. Note that this formulation also encompasses the case that one or more sources are independent of each other and from all the others; these sources can be coded with a classical AC, taking $\mathcal{A}_j = \emptyset$ for this source.

The selection of the sets \mathcal{A}_j and the overlap factors $k^{(j)}$, for $j = 1, \dots, P$, is still somewhat arbitrary, as the expected rate of source j depends on both the cardinality of \mathcal{A}_j and the value of $k^{(j)}$. In a realistic application it would be more practical to fix the sets \mathcal{A}_j once and for all, and to modify the parameters $k^{(j)}$ so as to obtain the desired rate. This is because, for time-varying correlations, one has to update the rate on-the-fly. In a distributed setting, varying one parameter $k^{(j)}$ requires to communicate the change only to source j , while varying the sets \mathcal{A}_j requires to communicate the change to all sources. Therefore, we define \mathcal{A}_j such that the P statistically dependent sources take in turns the role of the side information. Any additional independent sources are coded separately using $\mathcal{A}_j = \emptyset$. In particular, we set $\mathcal{A}_j = \{k | k \% P = j\}$, where $\%$ denotes the remainder of the division between two integers, and $0 \% j = 0$. The DAC encoder for the j -th source inserts ambiguity only at time instants $i \in \mathcal{A}_j$. At each node, the decoder stores the states of the P arithmetic decoders, and possibly performs a branching if the codeword related to the only potentially ambiguous symbol at the current time i is actually ambiguous. Although this encoding and decoding structure is not necessarily optimal, it does lead to a viable decoding strategy.

VI. RESULTS: ASYMMETRIC CODING

In the following we provide results of a performance evaluation carried out on DAC. We implement a communication system that employs a DAC and a joint decoder, with no feed-back channel; at the decoder, pruning is performed using the M-algorithm [39], with $M=2048$. The side information is obtained by sending the source X through a binary symmetric channel with transition probability p , which measures the correlation between the two sources. We simulate a source with both balanced

($p_0 = 0.5$) and skewed ($p_0 > 0.5$) symbol probabilities. The first setting implies $H(X) = H(Y) = 1$ and $H(X, Y) = 1 + H(X|Y)$, where $H(X|Y)$ depends on p . The closer p to 0.5, the less correlated the sources, and hence the higher $H(X|Y)$. In the skewed case, given p_0 , $H(X)$ is fixed, whereas both $H(Y)$ and $H(X|Y)$ depend on p . Unless otherwise specified, each point of the figures/tables presented in the following has been generated averaging the results obtained encoding 10^7 samples.

A. Effect of termination

As a first experiment, the benefit of the termination policy is assessed. An i.i.d. stationary source X emits sequences \underline{x} of $N = 200$ symbols, with $p_0 = 0.5$ and $H(X|Y) = 0.25$, which are encoded with DAC at fixed rate 0.5 bps, i.e., 0.25 bps higher than the theoretical S-W bound. For Y we assume ideal lossless encoding at average rate $H(Y) = 1$ bps, so that the total average rate of X and Y is 1.5 bps. The bit error rate (BER) yielded by the decoder is measured for increasing values of the number of termination symbols T . The same simulation is performed with $N = 1000$. In all simulated cases, the DAC overlap has been selected to compensate for the rate penalty incurred by the termination, so as to achieve the 1.5 bps overall target rate. The overlap factors α_j^X are selected according to (6).

The results are shown in Fig. 4; it can be seen that the proposed termination is effective at reducing the BER. There is a trade-off in that, for a given rate, increasing T reduces the effect of errors in the last symbols, but requires to overlap the intervals more. It is also interesting to consider the position of the first decoding error as, without termination, errors tend to cluster at the end of the block. For $N = 200$, the mean position value is 191, 178, 168, 161 and 95, with standard deviation 13, 18, 25, 36 and 49, respectively for T equal to 0, 5, 10, 15 and 20. For $N = 1000$, the mean value is 987, 954, 881, 637 and 536, with standard deviation 57, 124, 229, 308 and 299. The optimal values of T are around 15-20 symbols. Therefore, we have selected $T = 15$ and used this value for all the experiments reported in the following.

B. Effect of the overlap design rule

Next, an experiment has been performed to validate the theoretical analysis of the effects of different overlap designs shown in Sect. IV-B. In Fig. 5 the performance obtained by using the design of equations (4) and (6) respectively is shown. The experimental settings are $N = 200$, $p_0 = 0.8$, fixed rate for \underline{x} of 0.5 bps, and total average rate for X and Y equal to 1.5 bps, with ideal lossless encoding of Y at rate $H(Y)$. The BER is reported as a function of the source correlation expressed in terms of $H(X, Y)$. It is worth noticing that the performance yielded by different overlap design rules are almost equivalent. Note that the rule in (6) consistently outperforms that in (4), confirming that this

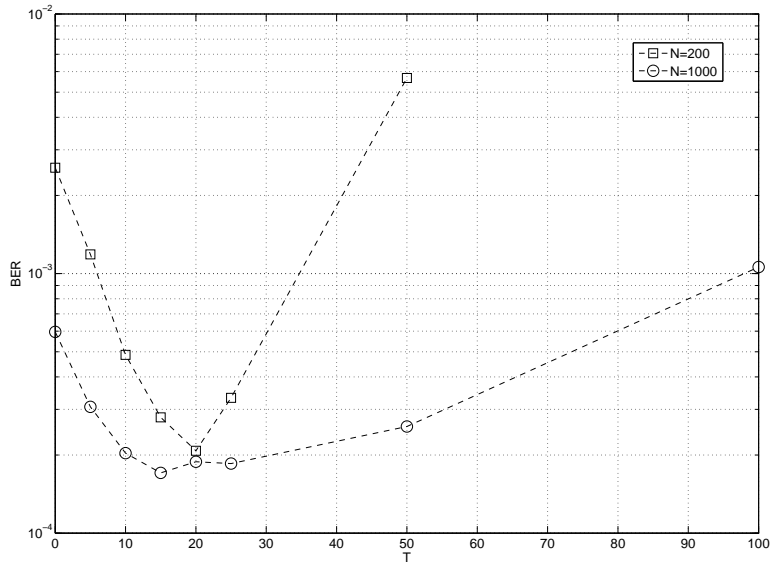


Fig. 4. BER as function of T (number of termination symbols); $p_0 = 0.5$, total rate = 1.5 bps, rate of $\underline{x} = 0.5$ bps, $H(X|Y) = 0.25$.

latter is only optimal for the rate. There is some difference when $H(X, Y)$ is very high (i.e., for weakly correlated sources). However, this case is of marginal interest since the performance is poor (the BER is of the order of 0.1).

C. Performance evaluation at fixed rate

The performance of the proposed system is compared with that of a system where the DAC encoder and decoder are replaced by a punctured turbo code similar to that in [6]. We use turbo codes with rate- $\frac{1}{2}$ generator (17,15) octal (8 states) and (31,27) octal (16 states), and employ S-random interleavers, and 15 decoder iterations. We consider the case of balanced source ($p_0 = p_1 = 0.5$) and skewed source (in particular $p_0 = 0.9$ and $p_0 = 0.8$). For a skewed source, as an improvement with respect to [6], the turbo decoder has been modified by adding to the decoder metric the *a priori* term, as done in [16]. Block sizes $N = 50$, $N = 200$ and $N = 1000$ have been considered (with S-random interleaver spread of 5, 11 and 25 respectively); this allows to assess the DAC performance at small and medium block lengths. Besides turbo codes, we also considered the rate-compatible LDPC codes proposed in [21]. For these codes, a software implementation is publicly available on the web; among the available pre-designed codes, we used the matrix for $N = 396$, which is comparable with the block lengths considered for the DAC and the turbo code.

The results are worked out in a fixed-rate coding setting as in [14], i.e., the rate is the same for each

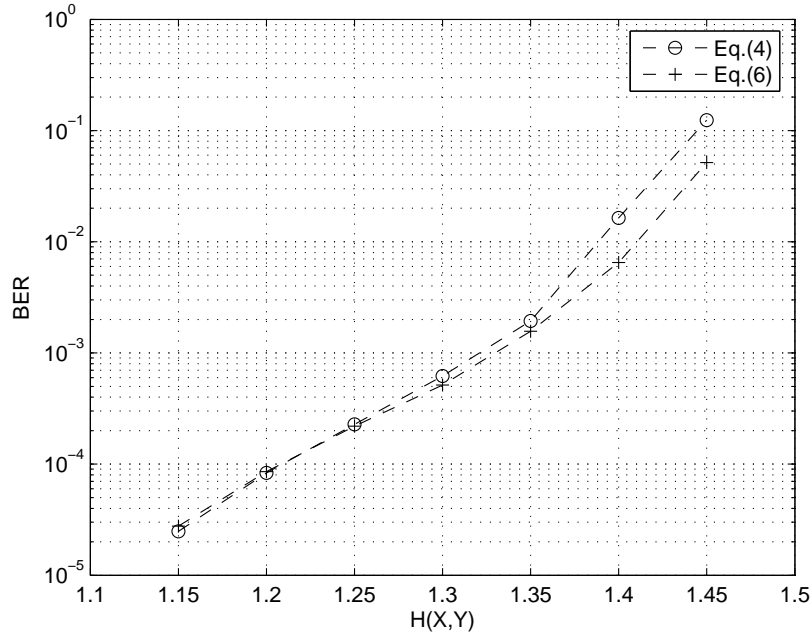


Fig. 5. Performance comparison between the use of different overlap rules ($p_0 = 0.8$, total rate = 1.5 bps).

sample realization of the source. Fig. 6 reports the results for the balanced source case; the abscissa is $H(X, Y)$, and is related to p . The performance is measured in terms of the residual BER after decoding, which is akin to the distortion in the Wyner-Ziv binary coding problem with Hamming metric. Both the DAC and the turbo code generate a description of \underline{x} at fixed rate 0.5 bps; the total average rate of X and Y is 1.5 bps, with ideal lossless encoding of Y at rate $H(Y)$. Since $H(Y) = 1$, we also have that $H(X, Y) = 1 + H(X|Y)$. This makes it possible to compare these results with the case of skewed sources which is presented later in this section, so as to verify that the performance is uniformly good for all distributions. The Wyner-Ziv bound for a doubly symmetric binary source with Hamming metric is also reported for comparison.

As can be seen, the performance of DAC slightly improves as the block length increases. This is mostly due to the effect of the termination. As the number of bits used to terminate the encoder is chosen independently of the block length, the rate penalty for non overlapping the last bits weights more when the block length is small, while the effect vanishes for large block length. In [34], where the termination effect is not considered, the performance is shown to be almost independent of the block size. It should also be noted that the value of M required for near-optimal performance grows exponentially with the block size. As a consequence, the memory which leads to near-optimal performance for $N = 50$ or $N = 200$ limits the performance for $N = 1000$.

We compared both 8-states and 16-states turbo codes. The 8-states code is often used in practical applications, as it exhibits a good trade-off between performance and complexity; the 16-states code is more powerful, and requires more computations. It can be seen that, for block length $N = 50$ and $N = 200$, the proposed system outperforms the 8-states and 16-states turbo codes. For block length $N = 1000$, the DAC performs better than the 8-states turbo code, and is equivalent to the 16-states code. It should be noted that, in this experiment, only the “channel coding performance” of the DAC is tested, since for the balanced source no compression is possible as $H(X) = 1$. Consequently, it is remarkable that the DAC turns out to be generally more powerful than the turbo code at equal block length. Note that the performance of the 16-states code is limited by the error floor, and could be improved using an ad-hoc design of the code or the interleaver; the DAC has no error floor, but its waterfall is less steep. For $H(X|Y) \geq 0.35$, a result not reported in Fig. 6 shows that the DAC with $N = 200$ and $N = 1000$ also outperform the 8-state turbo-coder with $N = 5000$. In Fig. 6 and in the following, it can be seen that turbo codes do not show the typical cliff-effect. This is due to the fact that, at the block lengths considered in this paper, the turbo code is still very far from the capacity; its performance improves for larger block lengths, where the cliff-effect can be seen. In terms of the rate penalty, setting a residual BER threshold of 10^{-4} , for $N = 200$ the DAC is almost 0.3 bps away from the S-W limit, while the best 16-state turbo code simulated in this paper is 0.35 bps away; for $N = 1000$ the DAC is 0.26 bps away, while the best 8-state turbo code is 0.30 bps away. The performance of the LDPC code for $N = 396$ is halfway between the turbo codes for $N = 200$ and $N = 1000$, and hence very similar to the DAC.

The results for a skewed source are reported in Fig. 7 for $p_0 = 0.8$. In this setting, we select various values of $H(X, Y)$, and encode \underline{x} at fixed rate such that the total average rate for X and Y equals 1.5 bps, with ideal lossless encoding of Y at rate $H(Y)$. For Fig. 7, from left to right, the rates of \underline{x} are respectively 0.68, 0.67, 0.66, 0.64, 0.63, 0.61, 0.59, and 0.58 bps. Consistently with [30], all turbo codes considered in this work perform rather poorly on skewed sources. In [30] this behavior is explained with the fact that, when the source is skewed, the states of the turbo code are used with uneven probability, leading to a smaller equivalent number of states. On the other hand, the DAC has good performance also for skewed sources, as it is designed to work with unbalanced distributions. The performance of the LDPC codes is similar to that of the best turbo codes, and slightly worse than the DAC.

Similar remarks can be made in the case of $p_0 = 0.9$, which is reported in Fig. 8. In this case, we have selected a total rate of 1 bps, since the source is more unbalanced and hence easier to compress. The rates for \underline{x} are respectively 0.31, 0.34, 0.37, 0.39, 0.42, 0.44, and 0.47 bps. In this case the turbo code performance is better than in the previous case, although it is still poorer than DAC. This is due

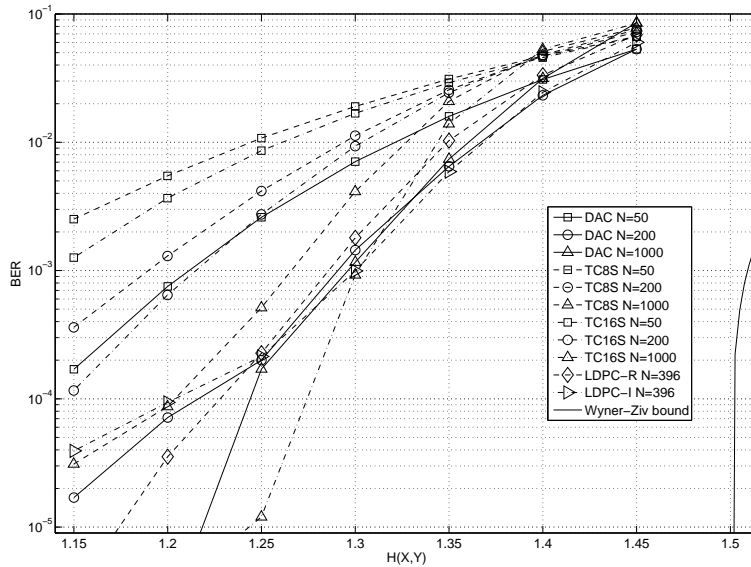


Fig. 6. Performance comparison of data communication systems ($p_0 = 0.5$, total rate = 1.5 bps, rate for $\underline{x} = 0.5$ bps): DAC versus turbo coding, balanced source. DAC: distributed arithmetic coding; TC8S and TC16S: 8- and 16-state turbo code with S-random interleaver; LDPC-R and LDPC-I: regular and irregular LDPC codes from [21].

to the fact that the sources are more correlated, and hence the crossover probability on the virtual channel is lower. Therefore, the turbo code has to correct a smaller number of errors, whereas for $p_0 = 0.8$ the correlation was weaker and hence the crossover probability was higher.

D. Performance evaluation for strongly correlated sources

We also considered the case of strongly correlated sources, for which high-rate channel codes are needed. These sources are a good model for the most significant bit-planes of several multimedia signals. Due to the inefficiency of syndrome-based coders, practical schemes often assume that no DSC is carried out on those bit-planes, e.g., they are not transmitted, and at the decoder they are directly replaced by the side information [9].

The results are reported in Tab. I for the DAC and the 16-state turbo code, when a rate of 0.1 bps is used for \underline{x} . The table also reports the cross-over probability p , corresponding, for a balanced source, to the performance of an uncoded system that reconstructs \underline{x} as the side information \underline{y} . As can be seen, the DAC has similar performance to the turbo codes and LDPC codes, and becomes better when the source is extremely correlated, i.e., $H(X|Y) = 0.001$.

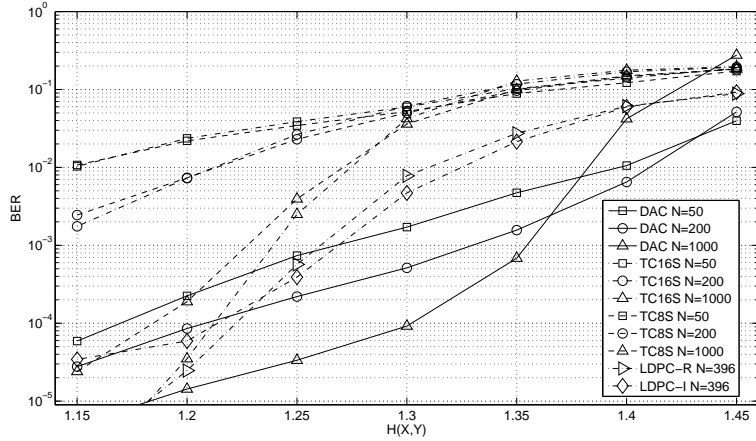


Fig. 7. Performance comparison of data communication systems ($p_0 = 0.8$, total rate = 1.5 bps): DAC versus turbo coding, skewed source. DAC: distributed arithmetic coding; TC8S and TC16S: 8- and 16-state turbo code with S-random interleaver; LDPC-R and LDPC-I: regular and irregular LDPC codes from [21].

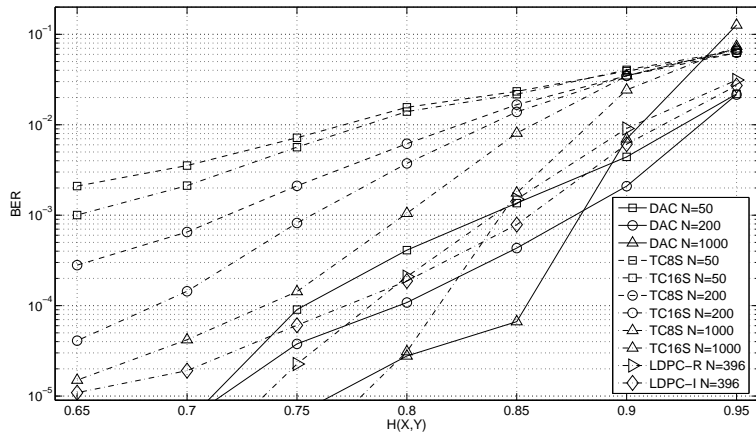


Fig. 8. Performance comparison of data communication systems ($p_0 = 0.9$, total rate = 1 bps): DAC versus turbo coding, skewed source. DAC: distributed arithmetic coding; TC8S and TC16S: 8- and 16-state turbo code with S-random interleaver; LDPC-R and LDPC-I: regular and irregular LDPC codes from [21].

E. Performance evaluation at variable rate

Finally, the coding efficiency of DAC is measured in terms of expected rate required to achieve error-free decoding. This amounts to re-encoding the sequence at increasing rates, and represents the optimal DAC performance if the encoder could exactly predict the decoder behavior. Since each realization of the source is encoded using a different number of bits, this case is referred to as variable-rate encoding. This scenario is representative of practical distributed compression settings,

TABLE I

RESIDUAL BER IN CASE OF STRONGLY CORRELATED SOURCES, WITH $p_0 = 0.5$ AND RATE FOR \underline{x} EQUAL TO 0.1 BPS.

$N = 200$			
$H(X Y)$	p	DAC	TC16S
0.1	$1.3 \cdot 10^{-2}$	$2.25 \cdot 10^{-2}$	$1.05 \cdot 10^{-2}$
0.01	$8.6 \cdot 10^{-4}$	$2.55 \cdot 10^{-4}$	$1.74 \cdot 10^{-4}$
0.001	$6.5 \cdot 10^{-5}$	$1.5 \cdot 10^{-6}$	$7.0 \cdot 10^{-6}$
$N = 1000$			
$H(X Y)$	p	DAC	TC16S
0.1	$1.3 \cdot 10^{-2}$	$2.10 \cdot 10^{-2}$	$1.18 \cdot 10^{-2}$
0.01	$8.6 \cdot 10^{-4}$	$1.5 \cdot 10^{-5}$	$2.9 \cdot 10^{-5}$
0.001	$6.5 \cdot 10^{-5}$	$< 1 \cdot 10^{-6}$	$1.0 \cdot 10^{-6}$
$N = 396$			
$H(X Y)$	p	LDPC-R	LDPC-I
0.1	$1.3 \cdot 10^{-2}$	$1.20 \cdot 10^{-2}$	$1.11 \cdot 10^{-2}$
0.01	$8.6 \cdot 10^{-4}$	$1.18 \cdot 10^{-4}$	$1.01 \cdot 10^{-4}$
0.001	$6.5 \cdot 10^{-5}$	$4.65 \cdot 10^{-6}$	$7.58 \cdot 10^{-6}$

e.g., [6], in which one seeks the shortest code that allows to reconstruct without errors each realization of the source process.

For this simulation, the following setup is used. The source correlation $H(X|Y)$ is kept constant and, for each sample realization of the source, the total rate is progressively increased beyond the S-W bound, in steps of 0.01 bps, until error-free decoding is obtained. This operation is repeated on 1000 different realizations of the source; the mean value and standard deviation of the rates yielding correct decoding are then computed.

The results have been worked out for block length $N = 200$, with probabilities $p_0 = 0.5$ and $p_0 = 0.9$. For $p_0 = 0.5$, the conditional entropy $H(X|Y)$ (i.e., the S-W bound) has been set to 0.5 bps. For $p_0 = 0.9$, the joint entropy $H(X, Y)$ has been set to 1 bps; this amounts to coding Y at the ideal rate of $H(Y) \simeq 0.715$ bps, with a S-W bound $H(X|Y) \simeq 0.285$ bps.

The results are reported in Tab. II. As can be seen, the DAC has a rate loss of about 0.06 bps with respect to the S-W bound for both the symmetric and skewed source. The turbo code exhibits a loss of about 0.2 bps and 0.13 bps. The LDPC-R code has a relatively small loss, i.e., 0.12 bps in the symmetric case and 0.10 in the skewed one. The LDPC-I code has a slightly smaller loss, i.e., 0.09 bps in the symmetric case and 0.075 in the skewed one. However, the DAC still performs slightly better. It should be noted that, while for LDPC and turbo codes the encoding is done only

once thanks to rate-compatibility, for the DAC multiple encodings are necessary, leading to higher complexity.

TABLE II

PERFORMANCE COMPARISON FOR VARIABLE-RATE CODING: MEAN AND STANDARD DEVIATION OF RATE NEEDED FOR LOSSLESS COMPRESSION.

	$p_0 = 0.5$		$p_0 = 0.9$	
$H(X Y), H(X, Y)$	0.50, 1.50		0.285, 1.0	
	mean	st.dev.	mean	st.dev.
DAC $N = 200$	0.56	0.04	0.32	0.03
LDPC-R $N = 396$	0.62	0.06	0.37	0.05
LDPC-I $N = 396$	0.59	0.06	0.35	0.05
TC16S $N = 200$	0.71	0.11	0.42	0.08
TC16S $N = 1000$	0.70	0.05	0.41	0.04

F. Performance versus complexity

As has been said, the DAC performance is a function of the block size and especially of the decoder parameter M . Tab. III reports comparative decoding results of DAC, turbo and LDPC codes for various values of M and N . The simulations have been made under the same conditions of Fig. 6, i.e. $p_0 = 0.5$, total average rate equal to 1.5 bps, and fixed rate of \underline{x} equal to 0.5 bps, considering the case of $H(X|Y) = 0.25$. Tab. III reports the residual BER, and the running time in milliseconds, obtained running the different decoders on a workstation with Pentium IV 3 GHz processor running Windows XP.

As can be seen, the DAC complexity grows exponentially with M . Increasing M typically improves performance, and the improvement is larger as N increases. Comparing DAC and turbo codes at approximately equal computation time, it can be seen that, for $N = 50$ and $N = 200$, the DAC performance is significantly better, while the turbo code outperforms DAC for $N = 1000$. For LDPC codes, the results for $N = 396$ can be compared with the DAC for $N = 200$. It can be seen that, with similar computation time, DAC and LDPC codes have similar performance. The BER yielded by the LDPC code is four times smaller than that of DAC, although it would increase going from $N = 396$ to $N = 200$.

VII. RESULTS: SYMMETRIC CODING

In the following we provide results for the symmetric DAC. We consider two sources with balanced ($p_0 = 0.5$) and unbalanced ($p_0 = 0.9$) distribution with arbitrary rate splitting, and use $M = 2048$.

TABLE III

DECODER COMPLEXITY AND PERFORMANCE FOR DAC, TURBO CODES AND LDPC CODES.

Algorithm	Parameter	BER	Time (ms)
DAC $N = 50$	$M = 64$	$1.20 \cdot 10^{-2}$	2.26
DAC $N = 50$	$M = 256$	$4.89 \cdot 10^{-3}$	9.64
DAC $N = 50$	$M = 512$	$3.49 \cdot 10^{-3}$	22.78
DAC $N = 50$	$M = 1024$	$2.93 \cdot 10^{-3}$	70.72
DAC $N = 50$	$M = 2048$	$2.61 \cdot 10^{-3}$	284.16
TC16S $N = 50$	15 iterations	$8.60 \cdot 10^{-3}$	9.30
DAC $N = 200$	$M = 64$	$3.15 \cdot 10^{-3}$	9.77
DAC $N = 200$	$M = 256$	$8.53 \cdot 10^{-4}$	44.96
DAC $N = 200$	$M = 512$	$4.55 \cdot 10^{-4}$	119.94
DAC $N = 200$	$M = 1024$	$2.80 \cdot 10^{-4}$	394.33
DAC $N = 200$	$M = 2048$	$2.00 \cdot 10^{-4}$	1538.43
TC16S $N = 200$	15 iterations	$2.74 \cdot 10^{-3}$	36.37
DAC $N = 1000$	$M = 64$	$5.36 \cdot 10^{-3}$	49.78
DAC $N = 1000$	$M = 256$	$1.06 \cdot 10^{-3}$	251.32
DAC $N = 1000$	$M = 512$	$5.25 \cdot 10^{-4}$	766.80
DAC $N = 1000$	$M = 1024$	$2.84 \cdot 10^{-4}$	2864.06
DAC $N = 1000$	$M = 2048$	$1.71 \cdot 10^{-4}$	11545.94
TC16S $N = 1000$	15 iterations	$1.2 \cdot 10^{-5}$	188.11
LDPC-R $N = 396$	100 iterations	$2.27 \cdot 10^{-4}$	16.95
LDPC-I $N = 396$	100 iterations	$2.14 \cdot 10^{-4}$	20.18

A. Performance evaluation at fixed rate

For fixed rate, we set the total rate of \underline{x} and \underline{y} equal to 1.5 bps. We consider two cases of rate splitting. In the first case the rate is equally split; we choose $k^X = k^Y$ so as to achieve a rate of 0.75 bps for each source. In the second case we encode \underline{x} at 0.6 bps and \underline{y} at 0.9 bps.

The performance of the symmetric DAC is worked out for $N = 200$ and $N = 1000$. Since symmetric DSC coders typically reconstructs each sequence either without any errors or with a large number of errors [28], we report the frame error rate (FER) instead of the residual BER, i.e. the probability that a data block contains at least one error after joint decoding. For each point, we simulated at least 10^7 bits.

Fig. 9 shows the results for the symmetric DAC. Comparisons with other algorithms can be done based on the following remarks. In [31], a symmetric S-W coder is proposed employing turbo codes, which can obtain any rate splitting. In the case that one source is encoded without ambiguity, this

reduces to the asymmetric turbo-based S-W coder we have employed in Sect. VI. In [31] it is reported that this algorithm achieves its best performance in the asymmetric points of the S-W region, while it is slightly poorer in the intermediate points. Therefore, in Fig. 9 we report the FER corresponding to the best turbo code shown in Fig. 6 for $N = 200$ and $N = 1000$, as this lower-bounds the FER achieved by [31] over the entire S-W region. Moreover, we also report the FER achieved by irregular LDPC codes with block length $N = 396$ [21]. The asymmetric algorithm in [21] has been extended in [33] to arbitrary rate splitting, showing that the performance is uniformly good over the entire S-W region. Finally, we also report the FER curve of the asymmetric DAC for $N = 1000$.

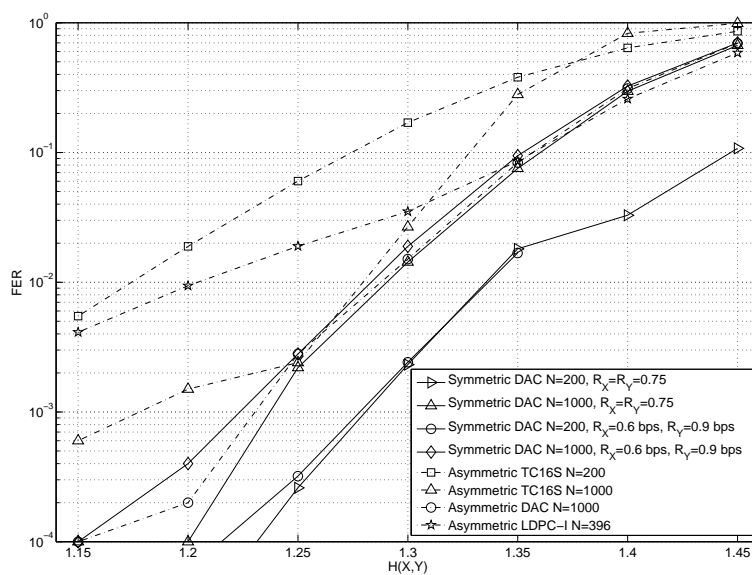


Fig. 9. Performance comparison of data communication systems ($p_0 = 0.5$, total rate = 1.5 bps). DAC: distributed arithmetic coding; TC16S: 16-state turbo code with S-random interleaver; LDPC-I: irregular LDPC codes from [21].

In Fig. 9, the results for symmetric coding are very similar to what has been observed in the asymmetric case. The DAC achieves very similar BER for $N = 200$ and $N = 1000$; hence, the FER is smaller for $N = 200$. The results are almost independent of the rate splitting between x and y , as can be seen by comparing the two rate-splitting cases as well as the asymmetric DAC. The turbo codes for $N = 200$ and $N = 1000$, and the irregular LDPC code, exhibit poorer performance than DAC.

B. Performance evaluation at variable rate

For variable rate coding, we consider the same two settings as in Sect. VI-E, i.e., block length $N = 200$, with probabilities $p_0 = 0.5$ and $p_0 = 0.9$; in the first case the conditional entropy has been

set to 0.5 bps, while in the second case the joint entropy $H(X, Y)$ has been set to 1 bps. The results are shown in Fig. 10. As can be seen, the performance of the symmetric DAC is uniformly good over the entire S-W region, and is significantly better than turbo codes and LDPC codes. In particular, the DAC suboptimality is between 0.03-0.06 bps, as opposed to 0.07-0.09 for the irregular LDPC code, and 0.14-0.21 for the turbo code. It should be noted, however, that variable rate coding requires feedback, while the S-W bound is achievable with no feedback, with vanishing error probability as $N \rightarrow \infty$. In our simulations we re-encode the sequence at increasing rates (in steps of 0.01 bps), which represents the optimal DAC performance if the encoder could exactly predict the decoder behavior.

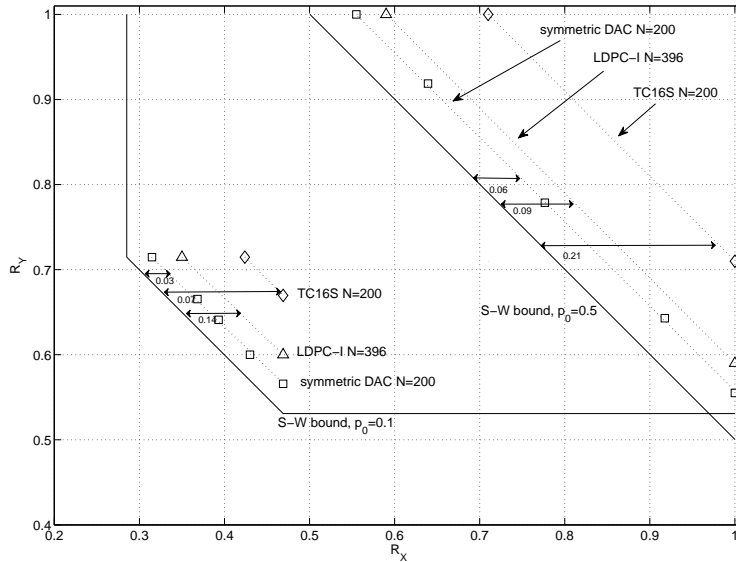


Fig. 10. Performance comparison at variable rate. The curves in the top-right corner refer to the case of $p_0 = 0.5$, and those in the bottom-left corner to $p_0 = 0.9$. DAC: distributed arithmetic coding; TC16S: 16-state turbo code with S-random interleaver; LDPC-I: irregular LDPC codes from [21]. The solid curves represent the S-W bound.

VIII. DISCUSSION AND CONCLUSIONS

We have proposed DAC as an alternative to existing DSC coders based on channel codes. DAC can operate in the entire S-W region, providing both asymmetric and symmetric coding.

DAC achieves good compression performance, with uniformly good results over the S-W rate region; in particular, its performance is comparable with or better than that of turbo and LDPC codes at small and medium block lengths. This is very important in many applications, e.g., in the

multimedia field, where the encoder partitions the compressed file into small units (e.g., packets in JPEG 2000, slices and NALUs in H.264/AVC) that have to be coded independently.

As for encoding complexity, which is of great interest for DSC, DAC has linear encoding complexity, like a classical AC [41]. Turbo codes and the LDPC codes in [21] also have linear encoding complexity, whereas general LDPC codes typically have more than linear, and typically quadratic complexity [42]. As a consequence, the complexity of DAC is suitable for DSC applications.

A major advantage of DAC lies in the fact that it can exploit statistical prior knowledge about the source very easily. This is a strong asset of AC, which is retained by DAC. Probabilities can be estimated on-the-fly based on past symbols; context-based models employing conditional probabilities can also be used, as well as other models providing the required probabilities. These models allow to account for the nonstationarity of typical real-world signals, which is a significant advantage over DSC coders based on channel codes. In fact, for channel codes, accounting for time-varying correlations requires to adjust the code rate, which can only be done for the next data block, incurring a significant adaptation delay. Moreover, with channel codes it is not easy to take advantage of prior information; for turbo codes it has been shown to be possible [43], employing a more sophisticated decoder.

Another advantage of the proposed DAC lies in the fact that the encoding process can be seen as a simple extension of the AC process. As a consequence, it is straightforward to extend an existing scheme employing AC as final entropy coding stage in order to provide DSC functionalities.

REFERENCES

- [1] D. Slepian and J.K. Wolf, "Noiseless coding of correlated information sources," *IEEE Transactions on Information Theory*, vol. 19, no. 4, pp. 471–480, July 1973.
- [2] A. Wyner and J. Ziv, "The rate-distortion function for source coding with side information at the decoder," *IEEE Transactions on Information Theory*, vol. 22, no. 1, pp. 1–10, Jan. 1976.
- [3] S.S. Pradhan, J. Chou, and K. Ramchandran, "Duality between source coding and channel coding and its extension to the side information case," *IEEE Transactions on Information Theory*, vol. 49, no. 5, pp. 1181–1203, May 2003.
- [4] R. Zamir, "The rate loss in the Wyner-Ziv problem," *IEEE Transactions on Information Theory*, vol. 42, no. 6, pp. 2073–2084, Nov. 1996.
- [5] R. Puri and K. Ramchandran, "PRISM: a "reversed" multimedia coding paradigm," in *Proc. of IEEE International Conference on Image Processing*, 2003, pp. 617–620.
- [6] B. Girod, A. Aaron, S. Rane, and D. Rebollo-Monedero, "Distributed video coding," *Proceedings of the IEEE*, vol. Special Issue on Advances in Video Coding and Delivery, no. 1, pp. 71–83, Jan. 2005.
- [7] M. Grangetto, E. Magli, and G. Olmo, "Context-based distributed wavelet video coding," in *Proceedings of IEEE International Workshop on Multimedia Signal Processing*, 2005.
- [8] C. Guillemot, F. Pereira, L. Torres, T. Ebrahimi, R. Leonardi, and J. Ostermann, "Distributed monoview and multiview video coding," *IEEE Signal Processing Magazine*, vol. 24, no. 5, pp. 67–76, Sept. 2007.
- [9] Q. Xu and Z. Xiong, "Layered Wyner-Ziv video coding," *IEEE Transactions on Image Processing*, vol. 15, no. 12, pp. 3791–3803, Dec. 2006.

- [10] H. Wang and A. Ortega, "Scalable predictive coding by nested quantization with layered side information," in *Proceedings of IEEE International Conference on Image Processing*, 2004, pp. 1755–1758.
- [11] A. Sehgal, A. Jagmohan, and N. Ahuja, "Wyner-Ziv coding of video: an error-resilient compression framework," *IEEE Transactions on Multimedia*, vol. 6, no. 2, pp. 249–258, Apr. 2004.
- [12] E. Magli, M. Barni, A. Abrardo, and M. Grangetto, "Distributed source coding techniques for lossless compression of hyperspectral images," *EURASIP Journal on Advances in Signal Processing*, vol. 2007, 2007.
- [13] N.-M. Cheung, C. Tang, A. Ortega, and C.S. Raghavendra, "Efficient wavelet-based predictive Slepian-Wolf coding for hyperspectral imagery," *Signal Processing*, vol. 86, no. 11, pp. 3180–3195, Nov. 2006.
- [14] Z. Xiong, A.D. Liveris, and S. Cheng, "Distributed source coding for sensor networks," *IEEE Signal Processing Magazine*, vol. 21, no. 5, pp. 80–94, Sept. 2004.
- [15] S.S. Pradhan and K. Ramchandran, "Distributed source coding using syndromes (DISCUS): Design and construction," *IEEE Transactions on Information Theory*, vol. 49, no. 3, pp. 626–643, Mar. 2003.
- [16] J. Garcia-Frias and Y. Zhao, "Compression of correlated binary sources using turbo codes," *IEEE Communications Letters*, vol. 5, no. 10, pp. 417–419, Oct. 2001.
- [17] A.D. Liveris, Z. Xiong, and C.N. Georghiades, "Distributed compression of binary sources using conventional parallel and serial concatenated convolutional codes," in *Proc. of IEEE Data Compression Conference*, 2003, pp. 193–202.
- [18] R. Gallager, *Low Density Parity Check Codes*, MIT Press, 1963.
- [19] A. Liveris, Z. Xiong, and C. Georghiades, "Compression of binary sources with side information at the decoder using LDPC codes," *IEEE Communications Letters*, vol. 6, no. 10, pp. 440–442, Oct. 2002.
- [20] Y. Yang, S. Cheng, Z. Xiong, and W. Zhao, "Wyner-Ziv coding based on TCQ and LDPC codes," in *Proceedings of Asilomar Conference on Signals, Systems, and Computers*, 2003, pp. 825–829.
- [21] D. Varodayan, A. Aaron, and B. Girod, "Rate adaptive codes for distributed source coding," *Signal Processing*, vol. 86, no. 11, pp. 3123–3130, Nov. 2006.
- [22] Z. Tu, J. Li, and R.S. Blum, "Compression of a binary source with side information using parallel concatenated convolutional codes," in *Proceedings of IEEE GLOBECOM*, 2004.
- [23] A. Majumdar, J. Chou, and K. Ramchandran, "Robust distributed video compression based on multilevel coset codes," in *Proceedings of Thirty-Seventh Asilomar Conference on Signals, Systems and Computers*, 2003, pp. 845–849.
- [24] S. Cheng and Z. Xiong, "Successive refinement for the Wyner-Ziv problem and layered code design," *IEEE Transactions on Signal Processing*, vol. 53, no. 8, pp. 3269–3281, Aug. 2005.
- [25] P. Koulgi, E. Tuncel, S.L. Regunathan, and K. Rose, "On zero-error source coding with decoder side information," *IEEE Transactions on Information Theory*, vol. 49, no. 1, pp. 99–111, Jan. 2003.
- [26] Q. Zhao and M. Effros, "Lossless and near-lossless source coding for multiple access networks," *IEEE Transactions on Information Theory*, vol. 49, no. 1, pp. 112–128, Jan. 2003.
- [27] S.S. Pradhan and K. Ramchandran, "Generalized coset codes for distributed binning," *IEEE Transactions on Information Theory*, vol. 51, no. 10, pp. 3457–3474, Oct. 2005.
- [28] V. Stankovic, A.D. Liveris, Z. Xiong, and C.N. Georghiades, "On code design for the Slepian-Wolf problem and lossless multiterminal networks," *IEEE Transactions on Information Theory*, vol. 52, no. 4, pp. 1495–1507, Apr. 2006.
- [29] N. Gehrig and P.L. Dragotti, "Symmetric and a-symmetric Slepian-Wolf codes with systematic and non-systematic linear codes," *IEEE Communications Letters*, vol. 9, no. 1, pp. 61–63, Jan. 2005.
- [30] P. Tan and J. Li, "A general and optimal framework to achieve the entire rate region for Slepian-Wolf coding," *Signal Processing*, vol. 86, no. 11, pp. 3102–3114, Nov. 2006.
- [31] J. Garcia-Frias and F. Cabarcas, "Approaching the Slepian-Wolf boundary using practical channel codes," *Signal Processing*, vol. 86, pp. 3096–3101, 2006.

- [32] M. Sartipi and F. Fekri, "Distributed source coding in wireless sensor networks using LDPC coding: The entire Slepian-Wolf rate region," in *Proceedings of IEEE WCNC*, 2005, pp. 1939–1944.
- [33] V. Toto-Zarasoá, A. Roumy, and C. Guillemot, "Rate-adaptive codes for the entire Slepian-Wolf region and arbitrarily correlated sources," in *Proceedings of IEEE ICASSP*, 2008, pp. 2965–2968.
- [34] M. Grangetto, E. Magli, and G. Olmo, "Distributed arithmetic coding," *IEEE Communications Letters*, vol. 11, no. 11, pp. 883–885, Nov. 2007.
- [35] M. Grangetto, E. Magli, and G. Olmo, "Symmetric distributed arithmetic coding of correlated sources," in *Proceedings of IEEE MMSP*, 2007, pp. 111–114.
- [36] X. Artigas, S. Malinowski, C. Guillemot, and L. Torres, "Overlapped quasi-arithmetic codes for distributed video coding," in *Proceedings of IEEE ICIP*, 2007, pp. 9–12.
- [37] P. Howard and J. Vitter, "Practical implementations of arithmetic coding," in *Image and Text Compression*. Norwell, 1992.
- [38] A. Moffatt, R.M. Neal, and I.H. Witten, "Arithmetic coding revisited," *ACM Transactions on Information Systems*, vol. 16, pp. 256–294, 1995.
- [39] J.B. Anderson and S. Mohan, *Source and Channel Coding*, Kluwer, 1991.
- [40] M. Grangetto, P. Cosman, and G. Olmo, "Joint source/channel coding and MAP decoding of arithmetic codes," *IEEE Transactions on Communications*, vol. 53, no. 6, pp. 1007–1016, June 2005.
- [41] H. Helfgott and M. Cohn, "Linear-time construction of optimal context trees," in *Proceedings of IEEE Data Compression Conference*, 1998, pp. 369–377.
- [42] T.J. Richardson and L.R. Urbanke, "Efficient encoding of low-density parity-check codes," *IEEE Transactions on Information Theory*, vol. 47, no. 2, pp. 638–656, Feb. 2001.
- [43] J. Garcia-Frias and J.D. Villasenor, "Joint turbo decoding and estimation of hidden Markov sources," *IEEE Journal on Selected Areas in Communications*, vol. 19, no. 9, pp. 1671–1679, Sept. 2001.